ENGINEERING TRANSACTIONS • *Engng. Trans.* • **59**, 2, 67–84, 2011
Polish Academy of Sciences • Institute of Fundamental Technological Research (IPPT PAN)
National Engineering School of Metz (ENIM)

CORRELATION BETWEEN DYNAMIC MATERIAL BEHAVIOR AND ADIABATIC SHEAR PHENOMENON FOR QUENCHED AND TEMPERED STEELS

F. Pursche, L.W. Meyer

Nordmetall GmbH
Hauptstrasse 16, D-09221 Adorf / Erzg., Gmd. Neukirchen

Besides the common failure mechanism based on crack propagation, adiabatic shear failure results from a collapse mechanism, mainly at high deformation rates. This failure incorporates locally extreme high shear strains, but due to the small volume involved, it transpires in a macroscopic brittle manner. This paper deals with the description of the influence of material properties on adiabatic shear failure. In the literature, much information can be found, which supports the theory that some material properties influence the occurrence of adiabatic shear failure behavior in a positive or negative manner. The determination of propensity for the investigated steels was done through special biaxial dynamic compression-shear-test in a drop weight tower. The failure achieved in the test is only material-dependent. Furthermore, it was found, that the theory of Culver with the competing processes of work hardening and thermal softening is transferable on the tested materials in a qualitative manner. Additionally, it was determined that few material properties have a strong controlling effect on the adiabatic shear failure behavior and it is possible to determine a critical value for transition between sheared and non sheared areas. Moreover, it could define a functional correlation of the failed materials to certain properties. As a main result, the most important material property is the dynamic compression behavior at high temperature. The stress level of the material and the characteristic in dependence of temperature is decisive. Analytical considerations using high temperature behavior patterns confirm this influence. Additionally, hardness and strength at room temperature and the pure shear capability (hat-shaped specimen) are also important for the evaluation of adiabatic failure behavior.

1. Introduction

In addition to the common failure mechanism based on crack propagation effects, another failure mechanism exists; this additional failure mechanism, which occurs mainly at high deformation rates, is the adiabatic shear failure. This localized failure yields to a macroscopic brittle rupture and thereby, to a reduction in the energy consumption. This failure behavior occurs in various technical areas, such as machining, forging, blanking, ballistics (target and penetrator), crash, surface friction, and detonative loading. The adiabatic shear failure behavior is mainly exhibited in metallic materials, like steel, titanium or aluminium, although it can also appear at plastics, rocks or ceramics.

In the literature much information can be found which supports the theory that some material properties influence the adiabatic shear failure behavior in a positive or negative manner. Tresca [1] and Zener and Hollomon [2] have observed that the strength and the heat capacity, as well as the thermal softening of the materials, have an important influence on the adiabatic shear behavior. Nowadays it is known that a lower strain hardening coefficient [3–5], a lower strain rate dependence [6–7], a lower heat capacity or thermal conductivity [3–5], a lower grain size [3, 8] or a lower density of the material [7–9], promote the adiabatic shear failure behavior. Additionally, a high hardness [10–13], a high strength [3, 4, 14, 15], a high thermal softening [3–5], a high loading velocity [5, 8, 16], a high pre-deformation [3, 17], and a high specimen size [18], promotes the adiabatic shear failure behavior too. Furthermore, additional properties exist, for example initial temperature [19], hydrostatic stress state [20, 21], and tensile loading [4]. Even considering these factors, they may promote or inhibit adiabatic shear failure depending on the precise circumstances.

The question then arises: which material properties have the strongest influence on adiabatic shear failure for the investigated materials in this study? Observing and measuring the adiabatic shear failure behavior was accomplished through the performance of materials under different experimental tests, firstly with compression and compression-shear-loading. Furthermore, there is much discussion concerning high temperature compressive strength, the Culver-theory [22], analytical consideration and a description of the correlation between the material properties and the adiabatic failure behavior of the materials.

The aim of this study is to point out the material properties which have strong influence on the adiabatic shear failure behavior for high strength low-alloyed steels. Is it possible to find correlations and associated material properties? The next issue involves the validity of the Culver-theory on the observed materials and a discussion of the influence of high temperature behavior on the adiabatic failure process.

2. Adiabatic shear phenomena

The beginning of the adiabatic shear failure process is initiated by mutual displacement of material areas. This displacement is shown through the alignment of segregation lines in the vicinity of a transformed shear band in a certain quenched and tempered steel (Fig. 1).

This deformation process undergoes mainly of high deformation velocity and is locally concentrated. Because of the high strain rate, the generated heat due to the strain hardening cannot dissipate in the surrounding material; thus, a tem-

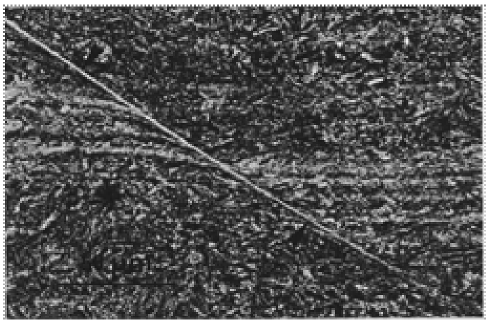

Fig. 1. Transformed shear band with segregation lines after DORMEVAL 1987.

perature rise will develop in the deformed region. Hence, a local temperature rise and a temperature gradient in the specimen, or in a component of the specimen, occur and manifest as a localized strength reduction. This process is further amplified and more localized, while further inducing a decrease in strength until the formation of an adiabatic shear band occurs and finally the failure appears.

The difference between the appearance of an adiabatic shear failure and the appearance of a classical fracture is shown in Fig. 2. In the classical fracture evaluation there is a differentiation from a brittle fracture compared to a ductile mixed and a pure ductile shear fracture. This ductile fracture is forced through shear stresses similar to the behavior under compression-shear-loading (Fig. 2 lower left). At very high loading rates, a local adiabatic deformation occurs and the rupture concentrates to low volumes, which is leading to brittle kind of fracture with low global, but high local energy consumption. The final result is comparable to the classical brittle fracture.

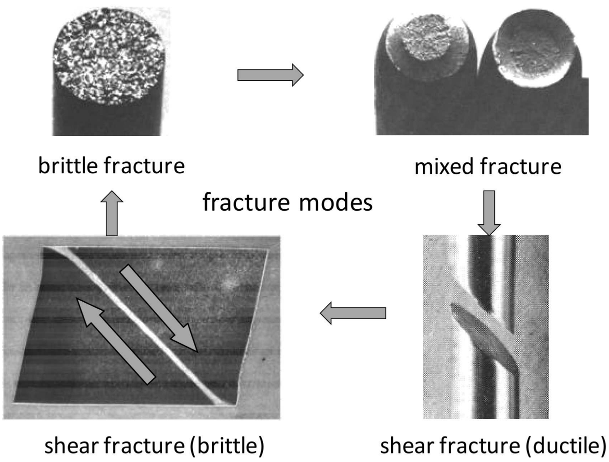

Fig. 2. Comparison of classical fracture modes to the adiabatic shear failure.

The investigations on adiabatic shear failure began in 1879 with Tresca [1]. He described the phenomenon of forging cross on a Pt-Ir-alloy and observed that a material's strength and heat capacity have an important influence on its adiabatic shear failure. In 1944, Zener and Hollomon [2] originated the theory of thermal instability due to the intense plastic deformation. Further research into the effects of strengthening and softening was conducted by Recht [23] in 1964 and Culver [22] in 1973. In the decades from the 1960s to the 1990s, investigations concerning the influence of the material behavior to the adiabatic shear failure were made by Rogers [24], Dormeval [4], Meyers [25], and Bai and Dodd [20]. In more recent years, studies of mechanical description have been made by Clifton [26] and Wright [27]. Additionally, studies of the microstructure of the initiation and development of shear bands have been performed by Meyers [28] and Xu [5].

Published literature contains a broad range of statements, which properties have an influence on the initiation of the adiabatic shear failure. These results can be divided into four groups. One group deals with the stress state (shear strength, shear strain, shear rate); a second group deals with the loading conditions such as temperature, stress state, energy or velocity. The third group deals with the microstructure of the material (precipitations, inclusions, voids etc.) and the fourth group describes the influence of the material properties such as density, heat capacity, strain hardening coefficient or thermal softening. The present study will be concentrated on the fourth group, material properties.

There are different assumptions for the critical condition of the beginning of the adiabatic shear failure. Most authors assume it is necessary to reach a certain amount of strain (Culver [22], Bai and Dodd [20] or Staker [29]). Other authors contend that a certain level of strain rate is crucial for the initiation of adiabatic shear bands (Recht [23] and Klepaczko [30]). Wang *et al.* [31] and Xu [5] describe a critical value as a consideration for strain and strain rate. Furthermore, there are assumptions that a critical energy must exist (Wang and Rittel [19]) or that a definite fracture toughness value are necessary (Grady [32]). Nowadays there are results that a dynamic recrystallization (called DRX) is responsible for the initiation condition [45, 46].

A well-known theory for describing of adiabatic shear failure is based on the principle from the work hardening and thermal softening of the material. These competing processes are described in a relation that shows the parts separately (Eq. (2.1)).

$$d\sigma = \left(\frac{\partial\sigma}{\partial\varepsilon}\right)_{\dot{\varepsilon},T} d\varepsilon + \left(\frac{\partial\sigma}{\partial\dot{\varepsilon}}\right)_{\varepsilon,T} d\dot{\varepsilon} + \left(\frac{\partial\sigma}{dT}\right)_{\dot{\varepsilon},\varepsilon} dT. \tag{2.1}$$

Adiabatic shear failure can occur, when the thermal softening of the material overcomes the strengthening due to the strain hardening and the strain rate hardening [4, 23, 25, 27]. The first term described the strain hardening, the second term – the strain rate hardening and the third term the thermal softening behavior, which acts against the first and second term. With the negligence of the second part and the differentiation with $d\varepsilon$, a criterion can be formulated for instability (Eq. (2.2); Recht [23], Culver [22], Bai and Dodd [20]):

$$\left(\frac{\partial\sigma}{\partial\varepsilon}\right)_{\dot{\varepsilon},T} + \left(\frac{\partial\sigma}{\partial T}\right)_{\dot{\varepsilon},\varepsilon} \frac{dT}{d\varepsilon} = 0. \tag{2.2}$$

The left term describes the influence of the strain hardening and the right term – the thermal softening behavior. The failure behavior can be imagined as a form of a convex adiabatic curve. When the equilibrium of both competing processes is reached, identical with the apex of the curve, an adiabatic shear failure can occur. From the above displayed softening theory Culver [22] has evolved a plain relation (Eq. (2.3)) to predict the failure strain of the material. Culver has made three assumptions. The strain hardening coefficient n_T from the isothermal behavior will substitute through the static one. The thermal softening behavior of the materials will remain linear and the stress relation (σ_T/σ_D) between dynamic isothermal and the dynamic adiabatic value will be neglected. Furthermore the density, the heat capacity and the Taylor-Quinney factor are contained.

$$\varepsilon_i = \frac{n_T \cdot \rho \cdot c_p}{0.9(\partial\sigma/\partial T)} \cdot \frac{\sigma_T}{\sigma_D}. \tag{2.3}$$

One objective of this study is to evaluate whether this theory from Culver is applicable to the investigated materials. The second objective of the examination, is to determine if there are additional material properties other than the thermal softening or hardness, which may influence the adiabatic shear failure behavior.

3. Test procedure and materials

Many different experimental methods exist to determine the propensity of a material to fail under adiabatic shear condition. Several test techniques are based on geometrical discontinuities, such as pure torsion [3, 4, 20, 27], hat-shaped [5, 27, 33, 40], single or double edge [16, 34], and punch loading [2, 3, 20, 43]. Alternatively, some techniques exist, where the failure is mainly dependent on the material behavior and is not initially influenced by geometry effects, such as compression [4, 27], compression-shear [35–37] or cylinder expansion test [5, 10, 20].

The determination of propensity for the investigated materials was done through a special biaxial dynamic compression-shear test at about 2 m/s in a drop weight tower, Fig. 3. The drop weight has a mass of 600 kg and can be stopped at desired displacement; thus, a visualization of development of adiabatic shear bands versus applied strains or from dark to white etching character is possible. This compression-shear specimen was invented by MEYER and STASKEWITSCH [39, 44] so that a wider differentiation of materials is available to contrast against the plain compression loading. For this reason the usual compression specimen is inclined a few degrees against the loading axis, with the effect of an enhanced multiaxial compression/shear loading. Depending on the desired amount of additional shear stresses, the inclination can be varied to max 10°. The specimens used in this study were 6° inclined. This little inclination will induce a certain biaxial compression-shear state in the specimen. Already this stress-state with only 10% of additional shear stresses challenges the material to fail with adiabatic shearing or not.

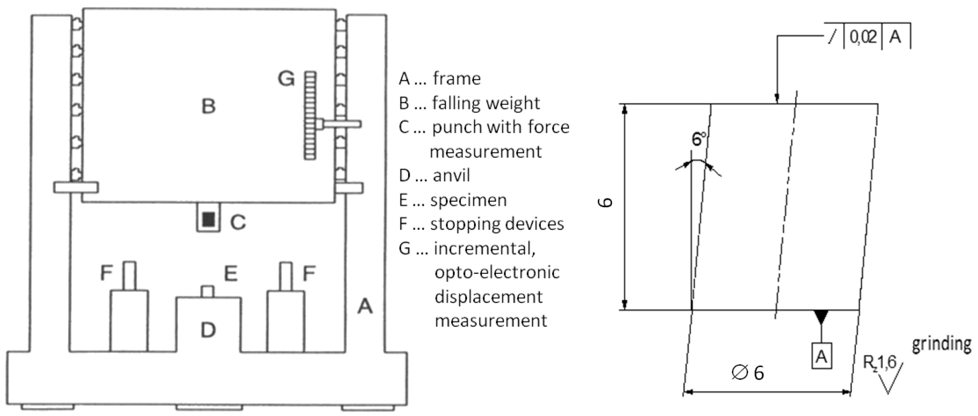

FIG. 3. Drop weight tower and test specimen.

The advantage of this technique is the absence of the influence of a stress enhancement like a surface flaw or a notch on the failure strain. The failure development is only dependent on the material's properties. As the first result of this test, it can be determined whether or not there is an occurrence of adiabatic shear failure. When shear failure occurs, a corresponding axial failure strain can be determined. Therefore, it is possible to give a qualitative and a quantitative result for an evaluation of the propensity of materials for adiabatic shear failure.

Additional tests were used for the determination of the correlations between material properties and adiabatic shear failure. Conducted were compression tests at room temperature and at high temperature, in order to measure the material's strength for the evaluation of the thermal softening of the materials. An often used technique is the use of the hat-shaped specimen, which was created by HARTMANN and MEYER [40]. The advantage of the hat-shaped test is that it can be used to test very ductile materials in a Compression-Setup such as SHPB or drop weight tower and a comparison between small and larger failure strain can be made. Tension tests were used for static and dynamic (1 m/s) velocities with a rotating wheel to determine values of strength and ductility. Also hardness tests, Charpy impact and fracture toughness tests were performed.

The materials used were several quenched and tempered steels with a broad range of hardness between 300 and 600 HB. The microstructure of the materials is a tempered martensitic structure.

4. Experimental results and discussion

Biaxial compression-shear tests were performed to verify the propensity to adiabatic shear failure of the materials. The specimens were tested at approximately 2 m/s with a drop weight device at room temperature. During the test the force and the displacement were both measured. A representative selection from all the materials with the axial engineering or technical compressive stress versus the axial technical strain is shown in Fig. 4 (left). It can be seen that two different behaviors exist. A few steels, with lower flow stresses, exhibit a more or less homogenous deformation until the limitation of displacement is reached. The other group of materials (about half of the investigated materials), shows sudden stress drop at lower strains. At this point the material failed due to adiabatic shearing. This measured amount of reduction for all failed materials was applied to determine additional correlations. It can be seen that exist different failure strengths and failure strains for the different steels. An initial consideration of the stress level shows that high strength steels are much more prone to adiabatic shear failure than the lower strength materials. This correlates to the hardness of the materials, Fig. 4 (right). With low hardness values, no adiabatic

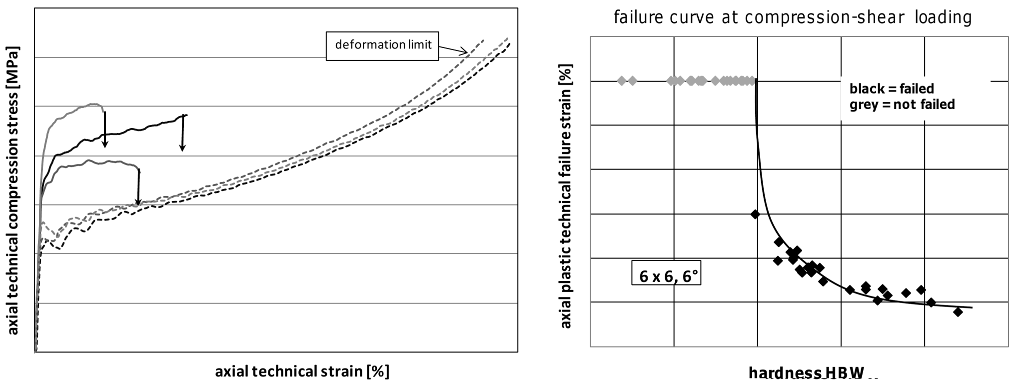

FIG. 4. Stress-strain behavior of the compression-shear test ($\dot{\varepsilon} = 200\ s^{-1}$) and the correlation with the hardness.

shear failure occurred. The grey points are defined at a deformation limit of the drop weight device. At certain hardness, first times adiabatic shear failure begins. As the material's hardness increases, the failure strain declines along with potential function. These results are valid for the materials and for the strain rate of $\dot{\varepsilon} = 200\ \mathrm{s}^{-1}$ investigated in this study. This dependence, already cited in the literature, is hereby confirmed.

The next examinations involve (pure) compression loading at room temperature. A selection of true stress-true strain-diagrams of the investigated materials at a strain rate of $\dot{\varepsilon} = 200\ \mathrm{s}^{-1}$ is shown in Fig. 5. The material behavior under this adiabatic condition begins at the lowest strength level with a pure strain hardening behavior, for example of a plain carbon steel. In the medium strength level, for example HSLA-steel, there an equilibrium between strain hardening and softening is existing. At the highest strength level mainly a softening behaviour occurs. These flow stress variations, responding to the hardening or softening behavior under dynamic compression loading, are arranged after their amounts in Fig. 5 (right). It can be seen that materials with a strong decline are prone to fail through adiabatic shearing. On the other hand there is an area with positive values, i.e. a hardening behavior. These materials most likely do not fail. In the depicted middle range, no clear dependence between the decline or softening behavior and the adiabatic shear failure is found. Thus, a conclusion can be made that the plain decline behavior under adiabatic compression is not clearly correlated with the adiabatic shear failure, at least not for this particular quenchend and tempered material group. The strain hardening coefficient, even at a strain rate of 200 1/s, which shall have an important influence on the adiabatic failure behavior, as described in the literature, cannot be confirmed for this material steel group. There might be a tendency, but for most of the steels a clear relation cannot be drawn.

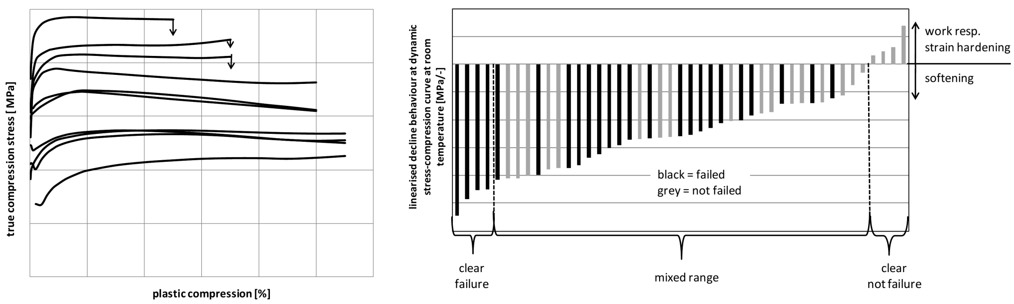

Fig. 5. True stress- true strain curves at (pure axial) dynamic compression ($\dot{\varepsilon} = 200\ \mathrm{s}^{-1}$) and results of softening determination.

The third investigation was to determine the stress behavior at high temperature under dynamic compression loading. The first result exhibits the different strength levels of the different steels, Fig. 6 (left). This distinct difference in flow stress lasts until about 600°C. With higher flow stress, the propensity to adiabatic shear failure is increased (arrow in Fig. 6). Materials with a high strength at room and at elevated temperatures are prone to adiabatic shearing. Furthermore, these materials show a rapid loss of strength with increased temperature. These drops of strength yield a development of a gradient of temperature-dependent stress resistance. This gradient is considerably higher for high strength steels. For low strength steels, the gradient is hardly sensible, and therefore these steels are not prone to adiabatic shearing, for example valid for the three curves depicted with no failure in Fig. 6. The results of the determined values of the linearized decline behavior at the stress-temperature-curves between temperatures of −100°C and 750°C is shown in Fig. 6 (right). There is a good correlation of the normalized strength decline value to the occurrence of adiabatic shear failure under compression shear loading. The stronger the decline behaviour, the lower the failure strain under compression-shear-loading will be. Above a certain value, no more failure occurred.

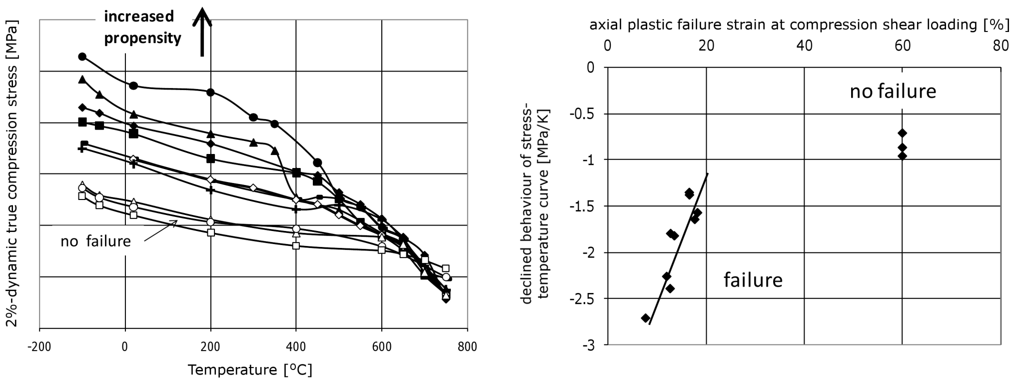

Fig. 6. Dynamic 2%-flow compression stress vs. starting temperature and determined declined flow stress values at dynamic strain rate of ($\dot{\varepsilon} = 200\ \mathrm{s}^{-1}$) between −100°C and 750°C.

The determined failure strains according to Culver (Eq. (2.3)) show a good qualitative correlation, Fig. 7. All materials with low calculated failure strain fail under compression-shear loading too. High values correlate with the materials with no failure. The depicted transition state is in the limit range of the used compression-shear loading test configuration. For the failed states, the correlation between the experimental and the calculated failure strain, Fig. 7 (right), show an absolute insufficient agreement. Thus, according to Culver for the investigated materials, it is only possible that a qualitative correlation with the softening theory exists.

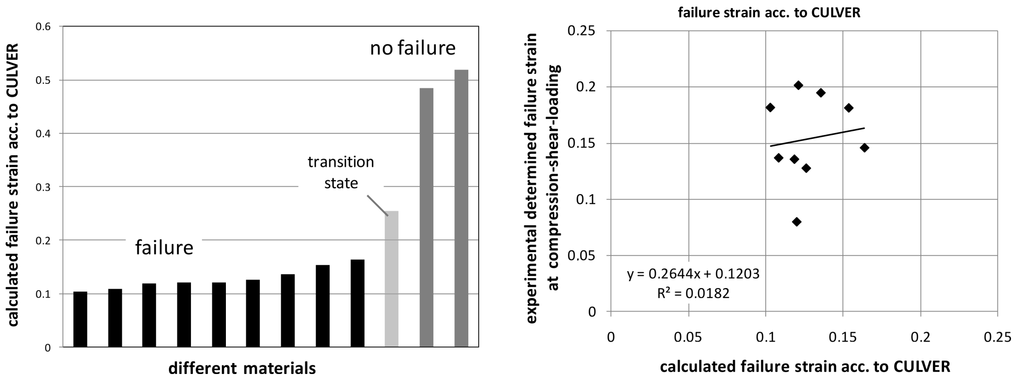

FIG. 7. Qualitative and quantitative evaluation of the materials using Culver-theory.

In addition to the previous examinations, stress-temperature-characteristics were also considered. Two examples of dynamic flow compression stress versus temperature are shown in Fig. 8. The left material shows a distinctive drop in strength; the right material shows at a certain temperature a change in the decline behavior. These points represent a change in the softening behavior from a low to high or higher decrease. These points are called "instability points" and from this, the related temperatures and stress values are obtained.

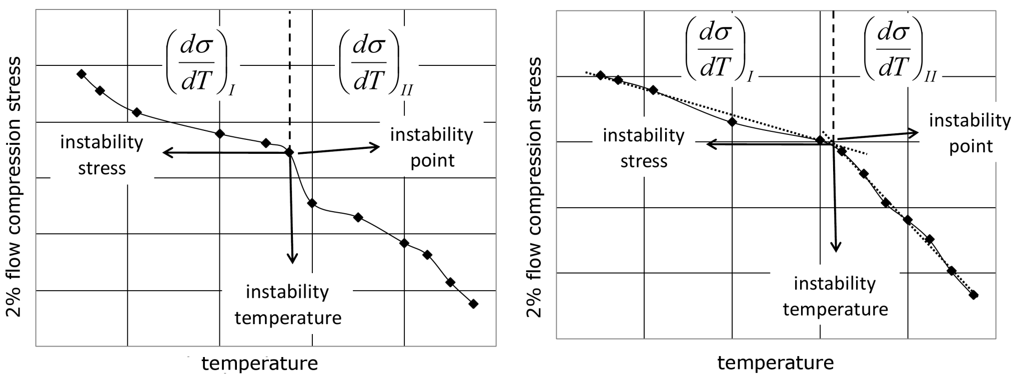

FIG. 8. Examples for determined instability points from dynamic flow compression stress vs. temperature ($\dot{\varepsilon} = 200\ \mathrm{s}^{-1}$).

The instability temperatures were correlated with the failure strain at compression-shear loading (Fig. 9, left). In the sheared area is a linear agreement with higher failure strain a higher instability temperature is determined. Above the instability temperature of 600°C there is no more failure. The determined instability temperatures and stresses for all materials were then depicted, Fig. 9 (right). With lower instability temperature and higher instability stress, the propensity to adiabatic shear failure increases. These results show that the spe-

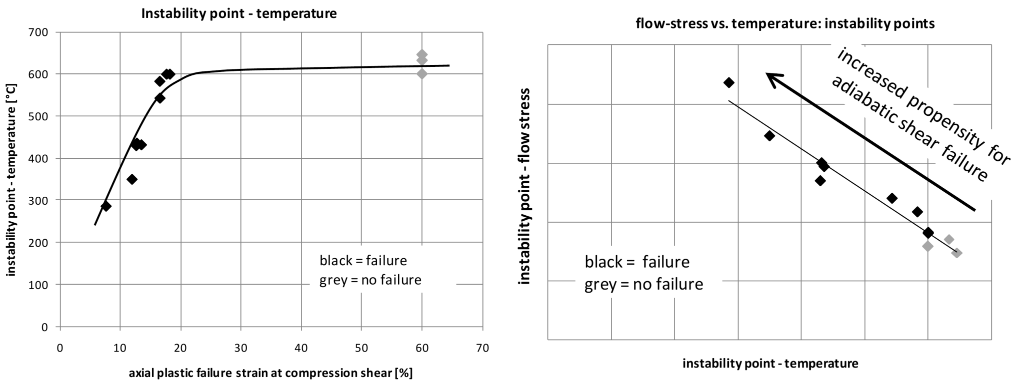

Fig. 9. Instability points of temperature versus failure strain at compression-shear loading and correlation of instability temperatures and stresses for all materials.

cific stress-temperature characteristic of the materials, especially the "instability points", from this study is a very valuable information and that the use of linearized decrease behavior is not always sufficient.

Previous results prove that the dynamic high temperature behavior of the materials is important for the evaluation of the propensity of adiabatic shear failure. The measured compression flow stress behavior at elevated temperatures was used to study the stress-strain-temperature-field analytically. The assumption (Fig. 10) is that the stress is a function of temperature, the temperature is a function of strain, and the strain is a function of a local position. Considering slow shear deformation, there is normally a homogenous distribution of strain and thus a homogenous distribution of temperature and stress. In the case of

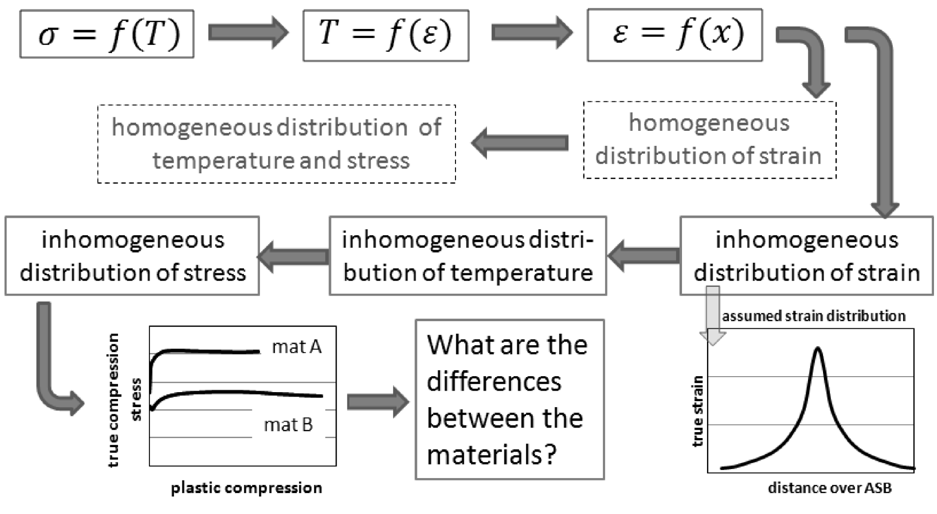

Fig. 10. Approach for the analytical consideration.

impact loading, an adiabatic deformation occurs. The related deformation field is inhomogeneous, like a strain distribution across the shear band, Fig. 10, lower right. This certain distribution yields an inhomogeneous distribution of temperature and stress (or a consequence). The used materials have different strength levels that evoke a different temperature rise in the specimen for the same deformation [41].

This different temperature behavior leads to a different stress resistance behavior, according to Feng and Bassim [42], across the shear band, Fig. 11 (left). Material A shows a considerable loss in stress resistance and thus a development of a strong gradient. This gradient is caused by the stress-temperature-behavior, similar to these in Fig. 8. This gradient leads to a local increased deformation and therefore to a local failure. Material B shows only a small loss of stress resistance; thus, this material is not susceptible to adiabatic shear failure. For the evaluation of the propensity to adiabatic shearing, the strength level and the intensity of the gradient are both important. From the analytically calculated temperature and stress gradient behaviors for all materials across the shear band, the minimum of stress resistance and the maximum of temperature (from the apex) was used to create a correlation between the calculated inner local temperature and inner stress resistance. These determined points show a linear dependence that with an increased local temperature, the propensity to adiabatic shear failure increases, Fig. 11 (right). After analytical consideration, these results confirm the conclusion that the stress-temperature behavior is important for the evaluation of the propensity of adiabatic shearing.

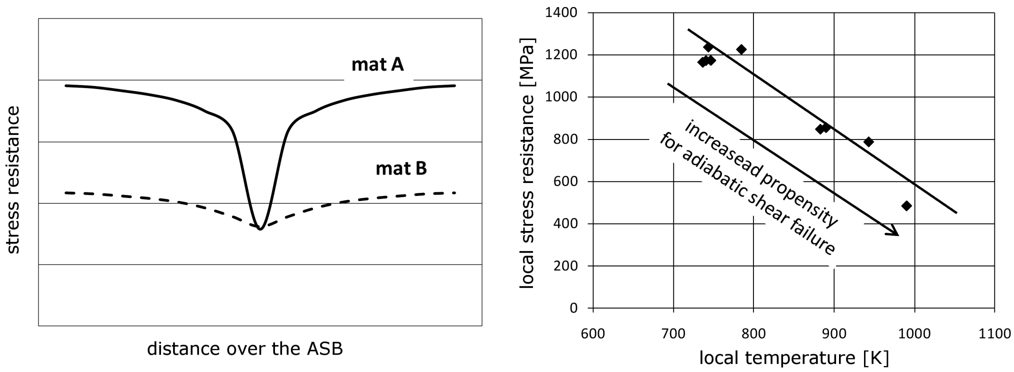

Fig. 11. Results of the analytic consideration and correlation to adiabatic shear failure.

Also interesting is the found result, that a correlation between the displacements, leading to failures, in the "hat" test and the inclined compression shear test, is existing. The failure strains at compression-shear loading correspond to the shear failure behavior at hat-shaped tests with a linear dependence, Fig. 12.

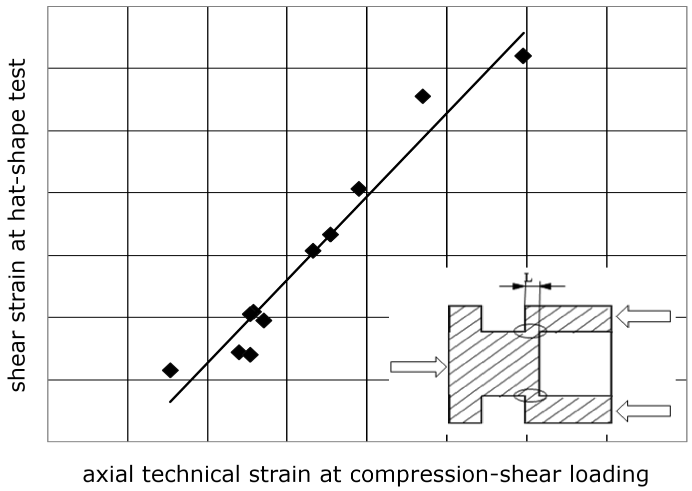

FIG. 12. Correlation of shear failure at hat-shape-test to the compression-shear failure.

This behavior is explained through the mutual influence of the mainly shear stress loading condition on the failure behavior for both test techniques.

For several material properties, a correlation to the adiabatic shear failure behavior was not found, like compression strain hardening coefficient at elevated temperatures, fracture strain and energy assumption at tensile loading, fracture toughness under mode I, and Charpy impact energy. As the reason, different loading conditions, which are not comparable and will lead to different failure modes, are assumed to be responsible.

GRADY [32] defined a shear fracture energy per unit area (Eq. (4.1)), which is necessary for initiation of shear band formation; surely, this approach is useable for the evaluation of materials for the propensity to adiabatic shear failure. In addition to Culver's theory, there are other properties involved such as thermal conductivity, flow shear stress and strain rate.

$$\Gamma = \frac{\rho \cdot c}{\alpha} \left(\frac{9 \cdot \rho^3 \cdot c^2 \cdot \chi^3}{\tau_y^3 \cdot \alpha^2 \cdot \dot{\varepsilon}} \right)^{1/4}, \tag{4.1}$$

where Γ – fracture energy per unit area, ρ – density, c – specific heat, χ – thermal conductivity, τ_y – flow shear stress, α – thermal softening, $\dot{\varepsilon}$ – strain rate.

With determined energy values (Fig. 13 left), a good differentiation to the tested materials is possible. Materials with a high amount of energy consumption correspond to the "no failure"-states and all materials with a low energy value failed under compression shear-loading. The difference between these two areas is considerable. Furthermore, in contrast to the theory of CULVER [22], there

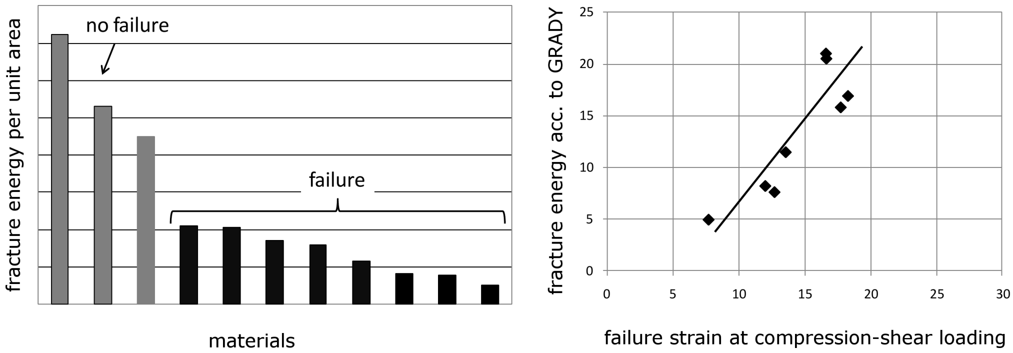

Fig. 13. Fracture energy acc. to Grady and the correlation to adiabatic compression-shear failure.

is a possibility of defining a quantitative correlation with the shear fracture energy of Grady [32]. This fracture energy, according to Grady, corresponds in a nearly linear agreement to the energy consumption until failure occurs at dynamic compression shear loading, Fig. 13 (right).

It is possible to summarise the results to an assessment, Fig. 14, because of the properties that give a correlation to the adiabatic shear failure behavior.

Property	Qualitative consideration	Quantitative consideration	Assessment rating
	threshold value	R^2-value	
instability point of **temperature** from dynamic stress-temperature-behavior	Yes	0.95	very good
shear failure from dynamic „hat"-shape-test	Yes	0.95	
instability point of **stress** from dynamic stress-temperature-behavior	Yes	0.94	
area under the dynamic stress-temperature-curve	Yes	0.94	
hardness	Yes	0.91	good
failure energy acc. to **GRADY**	Yes	0.87	
dynamic **compression flow stress** at room temperature	Yes	0.86	
dynamic **tensile strength** at room temperature	Yes	0.84	
decline behavior from dynamic compression-stress-temperature-behavior	Yes	0.79	
decline behavior from dynamic stress-compression-behavior of compression-shear-test	Yes	0.61	insufficient
uniform elongation under dynamic loading	Yes	0.47	
CULVER-equation	Yes	0.02	impossible

Fig. 14. Sensitive properties of adiabatic shear failure.

When a qualitative consideration is fulfilled, a quantitative consideration is then reasonable and an assessment rating is definable. With this assessment rating, a ranking of propensities to the adiabatic shear failure behavior can be determined. A threshold value for the transition between the areas of shear failure and no shear failure can be defined because of the qualitative correlations. When this correlation is in agreement without an overlapping of data, the correlation is then usable for an assessment. For the failed materials, it is possible to define a quantitative correlation. Because of the level of the least square coefficient R^2 of the agreement, it is possible to create a ranking of material properties according to their significance to the adiabatic shear failure behavior, Fig. 14.

A very good correlation to the occurrence of adiabatic shear failure behavior shows the instability point (determined at stress-temperature-behavior), the shear strain from hat shaped test, and the area under the stress-temperature-curve. These are the properties governed by the effect of temperature and shear deformation. Pertaining to hardness, the failure energy according to Grady, the dynamic compression flow stress, the dynamic tensile strength and the decline-behavior of the stress-temperature-curve, are all feasible to directly correlate to the adiabatic shear behaviour. These properties are based on hardness, energy consumption, and strength. It is notable that material properties exist, which exhibit a greater correlation to the adiabatic shear failure behavior than the material's hardness. The decline- or softening behavior of the stress-strain-curve under compression-shear-loading and the uniform elongation under dynamic tensile loading, give an insufficient correlation. The failure criterion according to Culver shows only a qualitative, but no good quantitative correlation.

5. Conclusion

The aim of this study was to examine the influence of material properties on the local adiabatic shear failure behavior. The test results of the investigated quenched and tempered steels allowed an evaluation of the materials concerning their adiabatic shear failure propensity. The determination of the failure strain under adiabatic condition was performed with special inclined compression specimens in a so-called compression-shear test. These dynamic tests were carried out in a drop weight tower with initial strain rates of 200 1/s.

The most important material property for the analysis of the adiabatic failure behavior is the temperature-softening characteristic of the material. Therefore the strength level and the stress drop characteristics are crucial. Eventually the so-called instability point can be defined. This value gives a good agreement to the measured failure strain under biaxial adiabatic shear condition. Analytical studies with the use of the determined dynamic stress-temperature-behavior confirmed (by means of development of the stress resistance gradient) the strong influence of the temperature softening behavior on the adiabatic shear failure.

The examined Culver-theory can only be used as a qualitative prediction for this material group. This theory is based on the linear softening behavior. The consideration of the shear fracture energy according to Grady gives both a qualitative as well as a good quantitative correlation to the measured shear failure behavior.

References

1. H. Tresca, *Sur la fluideite et lécoulement des corps solides*, Annales du conservatoire des arts et metiers, **41**, XI 1er fasc., 153–160, 1879.
2. C. Zener, J. H. Hollomon, *Effect of strain rate upon plastic flow of steel*, Journal of Applied Physics, **15**, 22–32, 1944.
3. H. C. Rogers, *Adiabatic shearing-general nature and material aspects, Material behavior under high stress and ultra-high loadings rates*, 29th Sagamore Army Materials Conf., J. Mescall and V. Weiss [Eds.], Plenum Press New York, Drexel University, Department of materials engineering, 101–118, 1983.
4. R. Dormeval, *The adiabatic shear phenomenon, Materials at high strain rates*, Elsevier Applied Science, T.Z. Blazynski [Ed.], 47–69, 1987.
5. Y. Xu, J. Zhag, Y. Bai, M. A. Meyers, *Shear localization in dynamic deformation: micro- structural evolution*, Metallurgical and Materials Transactions A, **39A**, 811–843, 2008.
6. R. Dormeval, *The adiabatic shear phenomena, Impact loading and dynamic behavior of materials*, Vol. 1, C. Y. Chiem, H. D. Kunze, L. W. Meyer [Eds.], DGM Informations-gesellschaft, Verlag, 43–56, 1988.
7. X. B. Wang, *Adiabatic shear localization for steels based on Johnson-Cook-Model and second- and fourth-order gradient plasticity models*, Journal of Iron and Steel Research, International, **14**, 56–61, 2007.
8. T. Pintat, B. Scholz, H. D. Kunze, O. Vöhringer, *The influence of carbon content and grain size on energy consumption during adiabatic shearing*, Journal de Physique, C3, **9**, 49, 237–244, 1988.
9. M. Edwards, *Properties of metals at high rates of strain*, Materials Science and Technology, **22**, 4, 453–462, 2006.
10. J. F. Mescall, *On the relative roles of strain-hardening and thermal softening in ASB*, Mechanical Engineering, Metallurgical application of shock-wave and high-strain-rate phenomena, **52**, 689–704, 1986.
11. J. Barry, G. Byrne, *Chip formation, acoustic emission and surface white layers in hard machining*, Annals of the CIRP, **51**, 65–70, 2002.
12. A. J. Bedford, A. L. Wingrove, K. R. L. Thompson, *The phenomenon of adiabatic shear deformation*, Journal of the Australian Institute of Metals, **19**, 1, 61–73, 1974.

13. Y. Meunier, R. Rouy, J. Moureaud, *Survey of adiabatic shear phenomena in armor steels with perforation*, Shock-wave and high strain rate phenomena in metals, 637–644, 1992.

14. A. G. Odeshi, S. Al-Ameeri, M. N. Bassim, *Effect of high strain rate on plastic deformation of a low alloy steel subjected to ballistic impact*, Journal of Materials Processing Technology, **162–163**, 385–391, 2005.

15. J. M. Yellup, R. L. Woodward, *Investigaion into the prevention of adiabatic shear failure in high strength armour materials*, Res. Mechanica, **1**, 41–57, 1980.

16. P. R. Guduru, A. J. Rosakis, G. Ravichandrian, *Dynamic shear bands: an investigation using high speed optical and infrared diagnostics*, Mechanics of Materials, **33**, 371–402, 2001.

17. A. Sabih, A. M. Elwazri, J. A. Nemes, S. Yue, *A workability criterion for the transformed ASB phenomena during cold heading of 1038 steel*, Journal of Failure and Prevention, **6**, 97–105, 2006.

18. N. Herzig, *Erfassung und Beschreibung des skalierten Fließ-, Verfestigungs- und Versagensverhalten ausgewählter metallischer Werkstoffe*, Dissertation, Schriftenreihe Band 004 Werkstoffverhalten, TU Chemnitz, Professur Werkstoffe des MB, 2008.

19. Z. G. Wang, G. Rittel, *Thermomechanical aspects of adiabatic shear failure of AM50 and Ti6Al4V alloys*, Mechanics of Materials, **40**, 8, 629–635, 2008.

20. Y. Bai, B. Dodd, *Adiabatic shear localization; Occurrence, theories and applications*, Pergamon press, Oxford, 1992.

21. E. Hanina, D. Rittel, Z. Rosenberg, *Pressure sensitivity of adiabatic shear banding in metals*, Applied physics letters, American institute of physics, **90**, 021915-1–021915-4, 2007.

22. R. S. Culver, *Thermal instability strain in dynamic plastic deformation*, Metallurgical effects at high strain rates, 519–529, 1973.

23. R. F. Recht, *Catastrophic thermoplastic shear*, Journal of Applied Materials, Transactions of the ASME, 189–193, 1964.

24. H. C. Rogers, *Adiabatic plastic deformation*, Ann. Rev. Mater. Sci., **9**, 283–311, 1979.

25. M. A. Meyers, *Dynamic behavior of materials*, Wiley-Interscience Publication; John Wiley and Sons, Inc., New York, 1994.

26. R. J. Clifton, *Material Response to ultra-high loadings rates*, Rep. NMAB - 356, NMAB, NAS, Washington, DC, Ch. 8, 1979.

27. T. W. Wright, *The physics and mathematics of ASB*, Cambridge University Press, 2002.

28. M. A. Meyers *et al.*, *Microstructural evolution in adiabatic shear localization in stainless steel*, Acta Materialia, **51**, 1307–1325, 2003.

29. M. R. Staker, *The relation between adiabatic shear instability strain and material properties*, Acta Metallurgica, **29**, 683–689, 1981.

30. J. R. Klepaczko, *Remarks on impact shearing*, Journal of Mechanics, Physics and Solids, **46**, 10, 2139–2153, 1998.

31. L. L. Wang, H. S. Bao, W. X. Lu, *The dependence of ASB in strain-rate, strain and temperature*, Journal de Physique, C3, **3**, 49, 207–214, 1988.

32. D. E. Grady, *Dissipation in adiabatic shear bands*, Mechanics of Materials, **17**, 289–293, 1994.

33. L. W. Meyer, L. Krüger, *Shear testing with hat specimen*, ASM Handbook, Mechanical Testing and Evaluation, ASM International, Materials Park, Ohio, **8**, 451–452, 2000.

34. J. F. Kalthoff, *Modes of dynamic shear failure in solids*, International Journal of Fracture, **101**, 1–31, 2000.

35. L. W. Meyer, L. Krüger, S. Abdel–Malek, *Adiabatische Schervorgänge*, Materialprüfung, **41**, 31–35, 1999.

36. L. W. Meyer, E. Staskewitsch, A. Burblies, *Adiabatic shear failure under biaxial dynamic compression/shear loading*, Mechanics of Materials, **17**, 203–214, 1994.

37. L. W. Meyer, L. Krüger, *Drop-weight compression shear testing*, ASM Handbook, Mechanical Testing and Evaluation, ASM International, Materials Park, Ohio, **8**, 452–454, 2000.

38. X. Sun, W. Liu, W. Chen, D. Templeton, *Modeling and characterization of dynamic failure of borosilicate glass under compression/shear loading*, Int. Journal of Impact Engineering, **36**, 226–234, 2009.

39. L. W. Meyer, E. Staskewitsch, *Adiabatic shear failure of the titanium alloy Ti6Al4V under biaxial dynamic compression/shear loading*, Shock Waves and high-strain-rate phenomena in metals, 1939–1946, 1992.

40. K. H. Hartmann, H. D. Kunze, L. W. Meyer, *Metallurgical effects on impact loaded materials*, Shock waves and high strain rate phenomena in metals, concepts and applications, Plenum Press New York, 325–337, 1981.

41. J. R. Klepaczko, B. Rezaig, *A numerical study of ASB in mild steel by dislocation mechanics based constitutive relations*, Mechanics of Materials, **24**, 125–139, 1996.

42. H. Feng, M. N. Bassim, *Finite element modeling of the formation of ASB in AISI 4340 steel*, Material Science and Engineering, **A266**, 255–260, 1999.

43. L. W. Meyer, S. Manwaring, *Critical adiabatic shear strength of low alloyed steel under compressive load*, Metallurgical applications of shock-wave and high-strain-rate phenomena, 657–674, 1986.

44. L. W. Meyer, *Adiabatic shear failure at biaxial dynamic compression/shear loading*, Euromech, **282**, 1991.

45. S. N. Medyanik, W. K. Liu, S. Li, *On criteria for dynamic adiabatic shear band propagation*, Journal of the Mechanics and Physics of Solids, **55**, 1439–1461, 2007.

46. L. E. Murr, *Applications of extreme deformation*, Materials Technology, **22**, 4, 193–199, 2007.

Received December 18, 2010; revised version May 31, 2011.